

GAS-FILLED MICROBUBBLES AS INTRAVASCULAR R_2^* CONTRAST AGENT FOR LIVER MRI

A. M. Chow^{1,2}, J. S. Cheung^{1,2}, A. Yu², H. Guo^{1,2}, and E. X. Wu^{1,2}

¹Laboratory of Biomedical Imaging and Signal Processing, The University of Hong Kong, Hong Kong SAR, China, People's Republic of, ²Department of Electrical and Electronic Engineering, The University of Hong Kong, Hong Kong SAR, China, People's Republic of

INTRODUCTION

Gas-filled microbubbles possess the potential to become a unique MR contrast agent because of their magnetic susceptibility effect, high biocompatibility and unique cavitation and sonoporation properties. However, *in vivo* demonstration of microbubble susceptibility effect is limited so far. In this study, we aim to further demonstrate and characterize the *in vivo* MR susceptibility effect induced by using both custom-made albumin-coated microbubbles (AMB) and commercially available lipid-based clinical ultrasound microbubble contrast agent (SonoVue®) in rat livers at 7 Tesla using dynamic susceptibility weighted MRI.

METHODS

Microbubbles Preparation: Air-filled AMBs were produced by sonication as previously described¹. SonoVue® microbubbles (Bracco) are commercially available, which consist of sulphur hexafluoride gas stabilized in aqueous dispersion by phospholipid monolayer. **Animal Procedures:** Normal SD rats (~250-350 g) ($N = 5$) were used. Femoral vein catheterization was performed with a 1-m long tube connected to a 27-gauge needle under anesthetization using IP injection of ketamine (100 mg/kg) and xylazine (10 mg/kg). The dead space in the catheter was about 0.2 mL. During MRI, animals were anesthetized with isoflurane/air using 1.0-1.5% via a nose cone. **Microbubbles Administration:** Microbubbles were first warmed slowly to room temperature and mixed to achieve uniform suspension. For each imaging session, 0.2 mL of microbubble suspension (~4% volume fraction for AMB and ~3.5% volume fraction for SonoVue®) was slowly injected at a rate of 1.2 mL/min to avoid possible microbubble destruction due to high pressure and shear stress. **MRI:** All MRI experiments were performed on a 7 T Bruker MRI scanner using a 60-mm quadrature RF coil. Anatomical images were acquired with 2D FLASH sequence with resolution = $0.20 \times 0.20 \times 2.0$ mm³. Dynamic susceptibility weighted liver MRI was performed with respiratory-gated single-shot GE-EPI sequence using TR \approx 1000 ms, TE = 10 ms, FA = 90°, FOV = 50 mm \times 50 mm, slice thickness = 2 mm, acquisition matrix = 64×64 , BW = 221 kHz and NEX = 1. To allow sufficient clearance of the microbubbles before the next injection, a minimum lapse of 10 min was used. The susceptibility effect of microbubbles was compared with that of a well-established intravascular contrast agent, monocrySTALLINE iron oxide nanoparticles (MION; MGH), by single dose of 0.6 mg Fe/kg injection using identical injection protocol and imaging sequence. **Image Analysis:** GE-EPI images were first co-registered using AIR5.2.5². ΔR_2^* maps were computed on a pixel-by-pixel basis as $\Delta R_2^* = \ln(S_{pre}/S_{avg-post})/TE$, where S_{pre} is the average intensity in 100 preinjection images and $S_{avg-post}$ is the average intensity in 40 postinjection images with maximum susceptibility contrast for microbubbles (or 100 postinjection images at steady-state contrast for MION). To quantify the ΔR_2^* values, ROIs were manually drawn in homogeneous liver region (LV) and the region covering inferior vena cava (IVC) based on the high resolution FLASH images. Assuming that ΔR_2^* is proportional to microbubble concentration $C(t)$ at time t , $C(t)$ can be estimated as $C(t) = k \ln\{S_{pre}/S(t)\}/TE + C_B$, where $S(t)$ is the image intensity at time t , k a proportionality constant, and C_B a constant residue to account for any postinjection baseline³. Given the relatively long injection time and the limited lifetime of microbubbles *in vivo*, $C(t)$ were approximately modeled with a gamma-variate function by curve fitting⁴. Full width at half maximum (FWHM) and time-to-peak were then measured from the fitted $C(t)$ time courses. **Ultrasound Demonstration:** Ultrasound imaging (Sonix RP, Ultrasonix) was performed in rat livers ($N = 2$) using SonoVue® to demonstrate microbubble induced contrast change for comparison.

RESULTS AND DISCUSSIONS

Figure 1(a) shows one of the preinjection GE-EPI T_2^* -weighted images, while (b) shows the postinjection GE-EPI T_2^* -weighted image with the maximum susceptibility contrast for AMB injection. Figure 2 depicts the typical T_2^* -weighted signal time courses during microbubbles injection with ROIs indicated in Figure 1(a). Two ROIs were selected from LV and IVC. The signal time course during SonoVue® injection captured by ultrasound imaging was overlaid in red for comparison. Note that the ultrasound signal was enhanced by microbubbles. Similar signal recovering patterns were observed, showing comparable lifetime of SonoVue® *in vivo*. The computed ΔR_2^* maps for AMB, SonoVue® and MION in the same animal were shown in Figure 3 and were found to be similar. However, the blood vessels in MION ΔR_2^* map were not as bright as those in microbubble ΔR_2^* maps, likely caused by the dominant T_1 shortening effect of MION at the low dosage used. Table 1 shows the *in vivo* measurements of the ΔR_2^* , FWHM and time-to-peak of AMB and SonoVue® as well as the ΔR_2^* and time-to-peak of MION in liver among all rats studied. The similar ΔR_2^* indicates that the *in vivo* susceptibility effects of AMB and SonoVue® at the dosage used are comparable to that of 0.6 mg Fe/kg MION in liver tissue at 7 T. However, time-to-peak was found to be shorter for MION. This is largely expected as microbubbles, with size comparable to that of red blood cells, flow slower than blood plasma while nano-sized MIONS flow together with plasma. In few of the rats studied (2 out of 5), the T_2^* -weighted signals after microbubble injection did not return to the preinjection baseline, this may be caused by microbubble trapping in local tissue vasculature. Possible uptake of intact microbubbles by Kupffer cells in liver may also contribute to such observation.

CONCLUSIONS

Substantial susceptibility induced changes were observed and characterized using gas-filled microbubbles for MRI at 7 T in rat livers, using custom-made albumin-coated microbubbles and a commercially available clinical ultrasound microbubble contrast agent. With the increasing availability of high-field MRI systems in both clinical and research setting, gas-filled microbubbles offer the promise as a viable intravascular contrast agent since their MR susceptibility effect increases⁵ with B_0^2 . With the unique cavitation and sonoporation characteristics, microbubble MRI has the potential for MRI guidance of microbubble-based drug delivery and therapies. Microbubble fabrication technology is also advancing. For example, substantially increased *in vivo* lifetime has been demonstrated recently using surfactant molecules with multiphase mixing technique⁶. Lastly, molecular targeting capability can also be achieved by microbubble surface modification⁷.

ACKNOWLEDGEMENTS

This work was supported by GRF7642/06M.

REFERENCES

[1] Cerny D, et al.; United States Patent 4957656. 1990. [2] Woods RP, et al., J Comput Assist Tomogr 1998;22(1):139-152. [3] Wong KK, et al., Magn Reson Med 2004;52(3):445-452. [4] Pickens DR, Invest Radiol 1992;27 Suppl 2:S12-17. [5] Dharmakumar R, et al., Magn Reson Med 2002;47(2):264-273. [6] Dressaire E, et al., Science 2008;320(5880):1198-1201. [7] Ferrara KW, Adv Drug Deliv Rev 2008;60(10):1097-1102.

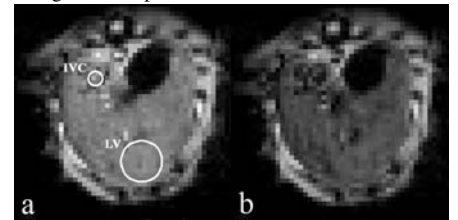


Figure 1 GE-EPI T_2^* -weighted image for AMB (0.2 mL of ~4% volume fraction) (a) preinjection image and (b) postinjection with the maximum susceptibility contrast.

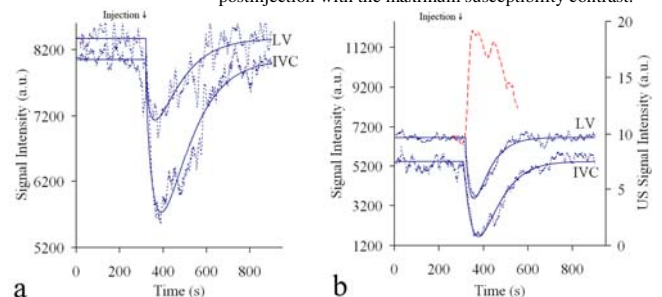


Figure 2 T_2^* -weighted signal time courses in different liver regions during (a) AMB and (b) SonoVue® injection in the same rat. Two ROIs for time course measurement, a homogenous liver region (LV) and the region covering inferior vena cava (IVC), are shown in Figure 1(a). Gamma-variate fitted data are shown in solid lines. Ultrasound measurement (red line) was overlaid in (b) for comparison.

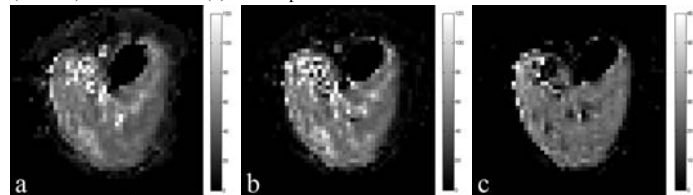


Figure 3 ΔR_2^* maps for (a) AMB, (b) SonoVue® and (c) 0.6 mg Fe/kg MION.

Table 1 Measurements of ΔR_2^* , FWHM and time-to-peak of the concentration time courses for AMB, SonoVue® and MION in rat liver (mean \pm standard deviation, $N = 5$).

	ΔR_2^* (s ⁻¹)	FWHM (s)	Time-to-peak (s)
AMB	40.89 \pm 22.08	119 \pm 68	60 \pm 24
SonoVue®	45.78 \pm 34.22	95 \pm 41	58 \pm 28
MION	55.84 \pm 21.75	N.A.	39 \pm 14